HHS Public Access

Author manuscript

EJC Paediatr Oncol. Author manuscript; available in PMC 2023 December 21.

Published in final edited form as:

EJC Paediatr Oncol. 2023 December ; 2: . doi:10.1016/j.ejcped.2023.100123.

The neonatal blood spot metabolome in retinoblastoma

Qi Yan[a,1], **Di He**[a,1], **Douglas I. Walker**[b], **Karan Uppal**[c], **Xuexia Wang**[d], **Helen T. Orimoloye**[e], **Dean P. Jones**[c,f], **Beate R. Ritz**[a,g], **Julia E. Heck**[a,e,*]

[a]Department of Epidemiology, UCLA Fielding School of Public Health, Los Angeles, CA, USA

[b]Gangarosa Department of Environmental Health, Rollins School of Public Health, Emory University, Atlanta, GA, USA

[c]Clinical Biomarkers Laboratory, Division of Pulmonary, Allergy, and Critical Care Medicine, School of Medicine, Emory University, Atlanta, GA, USA

[d]Department of Mathematics, University of North Texas, Denton, TX, USA

[e]College of Health and Public Service, University of North Texas, Denton, TX, USA

[f]Department of Medicine, Emory University, Atlanta, GA, USA

[g]Department of Neurology, UCLA School of Medicine, CA, USA

Abstract

Background: Retinoblastoma is rare but nevertheless the most common pediatric eye cancer that occurs in children under age 5. High-resolution metabolomics (HRM) is a powerful analytical approach to profile metabolic features and pathways or identify metabolite biomarkers. To date, no studies have used pre-diagnosis blood samples from retinoblastoma cases and compared them to healthy controls to elucidate early perturbations in tumor pathways.

Objectives: Here, we report on metabolic profiles of neonatal blood comparing cases later in childhood diagnosed with retinoblastoma and controls.

Methods: We employed untargeted metabolomics analysis using neonatal dried blood spots for 1327 children (474 retinoblastoma cases and 853 healthy controls) born in California from 1983 to 2011. Cases were selected from the California Cancer Registry and controls, frequency matched to cases by birth year, from California birth rolls. We performed high-resolution metabolomics to extract metabolic features, partial least squares discriminant analysis (PLS-DA) and logistic regression to identify features associated with disease, and Mummichog pathway analysis to characterize enriched biological pathways.

Results: PLS-DA identified 1917 discriminative features associated with retinoblastoma and Mummichog identified 14 retinoblastoma-related enriched pathways including linoleate

*Correspondence to: College of Health and Public ServiceUniversity of North Texas, 1155 Union Circle #311340, Denton, TX 76203-5017, USA. Julia.Heck@unt.edu (J.E. Heck).

[1]These authors contributed equally to this work as co-first authors.

Declaration of Competing Interest

The authors declare that they have no known competing financial interests or personal relationships that could have appeared to influence the work reported in this paper. All authors have declared no conflicts of interest.

metabolism, pentose phosphate pathway, pyrimidine metabolism, fructose and mannose metabolism, vitamin A metabolism, as well as fatty acid and lipid metabolism.

Interpretation: Our findings linked a retinoblastoma diagnosis in early life to newborn blood metabolome perturbations indicating alterations in inflammatory pathways and energy metabolism. Neonatal blood spots may provide a venue for early detection for this or potentially other childhood cancers.

Keywords

Retinoblastoma; Energy metabolism; Inflammation; Arachidonic acid; Tyrosine metabolism

1. Introduction

Retinoblastoma is the most frequent intraocular malignant tumor of childhood. It presents as hereditary (40%) or non-hereditary (60%). Hereditary cases are born with a constitutional mutation of the *RB1* gene, usually presenting with multiple bilateral tumors at an early age. However, only 6–10% of cases inherit a deleterious allele from an affected parent, while the remainder result from a de novo mutation in gametes [1]. Non-hereditary retinoblastoma results from the somatic inactivation of both *RB1* alleles in a single retinal progenitor cell, and its clinical presentation is typically unilateral and unifocal.

Even though *RB1* gene inactivation has been identified as the cause of retinoblastoma and its function has been elucidated, it is not well-known what triggers or contributes to the events that lead to retinoblastoma. High-resolution metabolomics (HRM) is a powerful approach that can profile thousands of endogenous and exogenous chemicals in biological specimens. Two untargeted metabolomics studies focused on retinoblastoma [2,3], both in populations of European descent that used tumor tissue to identify markers related to prognosis, differentiation, and tumor viability. They suggested involvement of the taurine/hypotaurine and glycerophospholipid (phosphocholine, glycerophosphocholine) pathways, with greater tumor differentiation related to higher taurine, and greater necrosis related to lipid, total taurine, creatine, hypotaurine, total choline, and phosphocholine [2]. Additional analyses that compared three embryonal tumor types observed that compared to neuroblastoma and medulloblastoma tissues, retinoblastoma tumor tissues have increased taurine, gamma-aminobutyric acid, creatine, lactate, and decreased glycine, phosphocholine, N-acetyl aspartate, aspartate and choline [3]. These observations are consistent with taurine being involved in photoreceptor development and conservation [4]. However, no studies used pre-diagnostic blood samples from retinoblastoma cases and compared them to samples from healthy controls to elucidate early markers of pathway perturbation that may contribute to the development of retinoblastoma. Here, we conducted an untargeted metabolomics study using newborn dried blood spot samples.

2. Materials and methods

Human subject permissions were obtained from the California Committee for the Protection of Human Subjects, the University of California Los Angeles, and the University of North Texas.

We utilized data from a population-based case-control study of childhood cancers among California children born 1983–2011 (ages ≤5 at diagnosis). Cases were identified from the California Cancer Registry, and controls were selected at random from California birthrolls and frequency matched (20:1) to cases by year of birth [5]. From this population, we randomly selected 1400 children (501 retinoblastoma cases and 899 controls) for HRM analysis.

Neonatal blood spots were collected by the California Genetic Disease Screening Program, as previously described [6]. We obtained demographic and gestational information from birth records.

After excluding 63 samples with missing covariates and 10 samples considered outliers based on metabolomic profiles, the present analysis included 474 retinoblastoma cases and 853 controls.

Blood spots were analyzed using liquid chromatography with ultra-high resolution mass spectrometry (LC-HRMS; Fusion, Thermo Scientific) following established methods [7]. Samples were punched using a 5 mm hole puncher and treated with 2:1 acetonitrile in water. Samples were mixed for 12 h at 0–4 °C in the dark and centrifuged to remove particulate matter. The resulting supernatant was analyzed in triplicate using hydrophilic interaction liquid chromatography (HILIC) with positive electrospray ionization (ESI) and C18 hydrophobic reversed-phase chromatography with negative ESI to enhance the coverage of metabolic feature detection. The mass spectrometer was operated using ESI mode at a resolution of 120,000 and a mass-to-charge ratio (*m/z*) range 85–1275. Raw data files were extracted and aligned using *apLCMS* with modifications by *xMSanalyzer*. Uniquely detected ions consisted of *m/z*, retention time, and ion abundance, referred to as metabolite features. Prior to data analysis, metabolite features were batch corrected using wavelet analysis [8]. For data analysis, we only included metabolomic features detected in > 80% of all blood spot samples, with median coefficients of variation (CV) among technical replicates < 30% and Pearson correlation > 0.7. Following quality assessment, replicate intensities were summarized using the median value, log2 transformed, and auto-scaled. Missing values were imputed using k-nearest neighbors (k = 10) provided in the *impute* R package.

We adopted a combination of univariate and multivariate analyses to identify neonatal blood metabolite features associated with later retinoblastoma, allowing us to discover biologically relevant metabolites while reducing the likelihood of false-positive findings [9]. Metabolite features that discriminated between cases and controls were selected by partial least square discriminant analysis (PLS-DA) with Variable Importance in Projection (VIP) scores > 1.5. PLS-DA is a supervised, multivariate analysis approach for dimensionality reduction that maximizes covariance between intensities of metabolic features and disease status [10]. In general, features with VIP score > 1 are considered important in a given model [11]. Ten-fold cross-validation and permutation tests were used to assess the performance of features selected by PLS-DA. Log2 fold change was calculated as the log2 transformation of the ratio between the metabolite abundance in the cases relative to the healthy controls. Logistic regression was used to assess associations between PLS-DA selected discriminative

metabolite features and retinoblastoma. Guided by the literature [5,12,13], we adjusted for maternal age (<20, 20–24, 25–29, 30–34, 35 +), maternal race/-ethnicity (White non-Hispanic, Hispanic of any race, other), birth year, gestational age (weeks), parity, infant's sex, foreign-born mother (Yes/No), and neighborhood socioeconomic status [14]. We accounted for multiple testing by using false discovery rate (FDR)-adjusted *p*-values. The majority (>90%) of sporadic bilateral cases involve a de novo mutation in the father's germline [15]. Therefore we additionally adjusted for paternal age and paternal education for bilateral analyses.

We conducted stratified analysis to investigate metabolomic changes related to unilateral and bilateral retinoblastoma separately. All analyses were performed using R 4.0.5.

Unilateral cases are often diagnosed at an older age than bilateral cases. To assess the influence of diagnosis age on neonatal metabolomic profiles for these two types of retinoblastoma, we restricted analyses to cases diagnosed before 18 months and further stratified by type. We conducted logistic regression analyses for each subgroup and calculated pairwise-*Pearson* correlations between the regression coefficients of metabolite features derived from any of the four strata.

To identify and annotate discriminative metabolite features, we used a combination of reference databases from the same HRM platform and through *xMSannotator*. HRM provides accurate mass (± 5 parts-per-million; ppm) measures of ion *m/z*, which can be related to chemical monoisotopic mass. Retinoblastoma-associated features were first matched to a reference database [16] of authenticated chemical standards (confidence level 1) from the same HRM platform. Additional metabolomic features not matching these metabolites were annotated using *xMSannotator*. Accurate mass *m/z* for adducts formed under positive/negative ESI mode was matched to the Human Metabolome Database with a mass error threshold of 5 ppm. *xMSannotator* uses a scoring system (0–3, a higher score representing a higher-confidence result) based upon correlation modularity clustering combined with isotopic, adduct, and mass defect grouping to improve the annotation of high-resolution mass spectrometry data. Only results with an annotation score > 2 were kept. The metabolite identification confidence levels [17] were reported for all annotation results.

To facilitate biological interpretation, we conducted pathway enrichment analysis using *mummichog* [18] to identify metabolic pathways associated with retinoblastoma. To account for all biologically relevant features and reduce type II error, metabolite features with PLS-DA VIP > 1.5 were included. Metabolites annotated by *mummichog* were required to be present in at least their primary adduct (M+H or M-H for positive and negative mode, respectively) to reduce the false positive match rate. Although annotation results in *mummichog* may include false positives, the enriched pathways inferred by the algorithm have been shown to be valid and to reflect real biological activity. A pathway was considered significant if gamma-adjusted *p*-values were smaller than 0.05. Only pathways that contained ≥ 3 discriminative metabolites were interpreted.

3. Results

Bilateral cases were diagnosed at 9.4 months of age (standard deviation (sd)= 8.6) and unilateral cases were diagnosed at 21.9 months (sd=14.6). Almost half of all mothers were of Hispanic origin (Table 1). Mothers of bilateral cases were older (35 + years) than control mothers.

3.1. Metabolic differences between all retinoblastoma cases and controls

We detected 16,739 metabolite features from the HILIC column coupled with the positive ionization mode (HILICpos) and 11,837 metabolite features from the C18 column coupled with the negative ionization mode (C18neg). After quality control, 17,018 metabolite features (10,188 HILICpos and 6830 C18neg) were included in analyses.

In adjusted analyses, PLS-DA identified 1917 discriminative features (1123 HILICpos features and 794 C18neg features) with VIP score > 1.5 (Fig. 1a–b). Out of the 1917 metabolite features, 51% were higher in abundance among retinoblastoma cases compared to controls. Subsequent logistic regression analysis revealed that 15 of these discriminative features had an FDR < 0.05. Approximately 16% of the metabolite features were tentatively annotated to one or more unique metabolite with medium or high confidence scores based on *xMSannotator* (confidence level 3). Annotation of top features included CMP-2-aminoethylphosphonate and pirbuterol (lower among cases) and N-acetyllactosamine and oligosaccharides (higher).

Mummichog analysis indicated that 14 metabolic pathways were differentially enriched with a permutation p-value < 0.05 (Fig. 1c, Supplemental Table 1). Top pathways included linoleate metabolism, pentose phosphate, pyrimidine, fructose and mannose metabolism, vitamin A, and fatty acid and lipid metabolism (glycerophospholipid metabolism, glycosphingolipid biosynthesis; Supplemental Table 2).

We matched the metabolites with previously confirmed chemical identities using MS2 spectra compared with authentic compounds analyzed under the identical experimental condition according to the Metabolomics Standards Initiative level 1 criteria. In total, we confirmed 28 metabolites (Table 2), including amino acids, nucleotides, and unsaturated fatty acids (9 of higher intensity among cases, and the rest lower). We confirmed docosahexaenoic acid (DHA) from the de novo fatty acid biosynthesis pathway to be higher among cases along with three other unsaturated fatty acids (adrenic acid, palmitoleic acid, and oleic acid) and all-trans-retinoic acids (ATRA), which is part of the Vitamin A (retinol) metabolism and involved in carcinogenesis [19].

3.2. Unilateral vs. bilateral cases

The comparison between unilateral cases and controls revealed 1873 discriminative features with VIP score > 1.5 (Supplemental Fig. 1). However, none of the discriminative features reached an FDR < 0.05. We identified 1830 discriminative features when comparing bilateral cases to controls (Supplemental Fig. 1) and logistic regression analysis revealed that 82 of these discriminative features had an FDR < 0.05. Out of all discriminative features identified, 202 overlapped across all three comparisons of which 9 were confirmed based on

authentic standards (Supplemental Figure 2a). Pathway enrichment analysis of overlapping features revealed that the pentose phosphate pathway, pyrimidine metabolism, fructose and mannose metabolism, and C5-branched dibasic acid metabolism were among the shared pathways associated with both unilateral and bilateral disease (Supplemental Figure 2b). A complete list of metabolite annotations within each pathway is provided in Supplemental Tables 3–4.

Unilateral and bilateral cases exhibited distinct metabolic signals relative to controls. We identified discriminative features involved in the tyrosine metabolism pathway, including hippuric acid and glutamine, to distinguish unilateral cases from controls. Metabolites uniquely related to bilateral cases included arachidonic acid and N-Acetylneuraminic acid (NANA), enriched in several pathways (linoleic acid metabolism, amino sugars metabolism, bile acid biosynthesis).

The mean age at diagnosis of bilateral RB is younger than that for unilateral RB (13 months vs. 25 months). When we further adjusted for age at diagnosis in the stratified analysis, results remained largely the same, suggesting that the distinct metabolites identified may point to inherent systemic metabolic differences in RB subtypes rather than confounding by diagnosis age.

4. Conclusions

Our analysis of neonatal blood spots showed that children later diagnosed with retinoblastoma exhibit metabolome perturbations in polyunsaturated fatty acid, nucleotide and sugar metabolism, the pentose phosphate and cofactor pathways, indicative of alterations in inflammatory pathways and energy metabolism.

We identified higher free polyunsaturated fatty acid levels (DHA, tetracosahexaenoic acid, eicosapentaenoic acid) among cases. DHA, the most abundant n-3 fatty acid in the nervous system, is required for neuronal regeneration and formation of synapses during fetal brain development. Only a small proportion of the n-3 fatty acids are of endogenous origin [20]. Long-chain polyunsaturated fatty acids are related to fish intake. Since 2002, DHA is a component of infant formula [21]. However, fatty acids are not only nutrients but also act as potent and specific blood-borne signaling molecules that accelerate or decelerate chemical reactions in cells [22]. Due to their hydrophobic nature, they are bound to albumin or present as fatty esters in lipoproteins, leaving only nanomolar amounts of free fatty acid in serum [23]. Thus, the free fatty acids we measured are most likely generated by phospholipase-dependent cell signaling events, many related to inflammatory responses.

Pathway enrichment analysis also identified fatty acid metabolism pathways associated with retinoblastoma suggesting oxidative stress and inflammation. In the linoleate pathway, linoleic acid and its downstream products 9(S)-HPOT and 13-keto-9Z,11E-octadecadienoic acid (13-oxo-ODE) were higher among cases. Linoleic acid can be catalyzed by lipoxygenase enzymes expressed by circulating immune cells to generate inflammatory mediators [24]. Inflammation contributes to Rb protein hyperphosphorylation, activating genes associated with cell proliferation and apoptosis inhibition [25]. Moreover, metabolic

alterations in oxidative stress and inflammatory pathways could arise from pesticide and air pollution exposures [26,27], and exposure to these pollutants has been associated with a higher risk of retinoblastoma [28,29]. Therefore, alterations in unsaturated fatty acid metabolic pathways may indirectly link environmental exposures during pregnancy and retinoblastoma through oxidative stress and inflammation.

Purines and pyrimidines are some of the most abundant metabolic substrates for all living organisms as they provide the essential components for DNA and RNA [30]. We observed a negative association between retinoblastoma and purine and pyrimidine nucleotides. Studies have shown that purines participate in immune responses and host–tumor interaction. Alterations of purine metabolites have been indicated in tumor cells [31], and imbalance in the gene expression pattern of purine metabolism enzymes was linked with tumor progression [32].

Retinoblastoma cases exhibited differences in features belonging to vitamin A metabolism: ATRA and retinol derivatives (14-hydroxy-4,14-retro-retinol, all-trans-5,6-epoxyretinoic acid, and 13,14-dihydroxy-retinol) were higher whereas anhydroretinol was lower compared to controls. The signaling molecule ATRA regulates the development of various tissues and is required for immune system function [33]. Retinol is the precursor for retinoids, which affect various aspects of morphogenesis and development [34]. Vitamin A modulates immune response through retinoic acid [35], and enables the redox activation of protein kinase Cδ (PCKδ) with cytochrome. The PCKδ signaling system, comprised of PKCδ, the adapter protein p66Shc, cytochrome c, and retinol, positively regulates the conversion of pyruvate to acetyl-coenzyme A (CoA) by the pyruvate dehydrogenase enzyme [36]. Vitamin A therefore plays a crucial role in glycolytic energy generation in the tricarboxyl acid (TCA) cycle. It is possible that perturbation of vitamin A metabolism indicates disturbances in energy metabolism and mitochondrial function that contribute to the development of retinoblastoma.

We identified several diabetes-related metabolites and metabolic pathways in our study, such as docosahexaenoic acid, O-phosphoethanolamine, and sugar metabolism. One previous study linked gestational diabetes with retinoblastoma [37] and another study suggested that gestational diabetes increases levels of oxidative DNA damage [38]. In the diabetic retina, hyperglycemia may lead to elevated oxidant production and damage [39].

A limitation is that we lack information on whether a retinoblastoma case is familial. Only 6–10% of retinoblastoma cases have a family history of the disease [40]. We stratified analyses by laterality as bilateral cases can be considered proxies for sporadic heritable cases. We found that alterations in the pentose phosphate pathway (PPP), important in glucose metabolism, are seen in both types whereas several metabolic signals are uniquely associated with either unilateral or bilateral cases. N-Acetylneuraminic acid (NANA) was found to have lower levels only among bilateral cases compared to controls. NANA is the most common form of sialic acid that plays a role in cell signaling, binding and transport of positively charged molecules, attraction and repulsion of cells and molecules, and immunity [41]. NANA has been previously reported as an agent that may protect cancer cells from immune surveillance [42], as sialylated conjugates protect malignant cancer cells from

cellular defense systems. Moreover, altered levels of NANA have been found in various cancer types [43], and sialic acid has been proposed as a tumor blood biomarker [44] For confounder control, we had a limited number of covariates from the birth certificate. We lacked information on maternal diet, environmental, or occupational exposures. However, this would not invalidate our results as these exposures can be conceptualized as contributing to the generation of the distinct metabolic features we identified in certain pathways i.e. features or pathways identified would be mediators of these agents' effects. Further studies are needed to identify such upstream factors that may have caused the observed metabolic differences. For example, we and others [27,45] previously identified air pollution as an exposure that perturbs the linoleate pathway and air pollution has been shown to contribute to retinoblastoma risk [28,29]. Another limitation is related to the still limited ability to annotate many metabolic features detected in an untargeted analysis. Adopting a pathway and network analysis approach, we were able to improve our annotations, but incorrect matches may have influenced the interpretation of our results.

In conclusion, we linked oxidative stress and inflammatory pathways to retinoblastoma and also identified some metabolites that have previously been linked to cancer cell evasion by the cellular immune system.

Supplementary Material

Refer to Web version on PubMed Central for supplementary material.

Acknowledgements

The biospecimens and data used in this study were obtained from the California Biobank Program (SIS request number 565). The California Department of Public Health is not responsible for the results or conclusions drawn by the authors of this publication.

Funding

This work was supported by grants from the US National Institutes of Health (R03CA252788, R21ES018960, R21ES019986); the California Tobacco-Related Disease Research Program of the University of California (24RT-0033H, T29DT0485).

Data Availability

Data availability is under the regulation of the California Committee for the Protection of Human Subjects.

References

[1]. Kato MV, Ishizaki K, Shimizu T, Ejima Y, Tanooka H, Takayama J, et al. , Parental origin of germ-line and somatic mutations in the retinoblastoma gene, Hum. Genet 94 (1994) 31–38. [PubMed: 8034292]

[2]. Kohe S, Brundler MA, Jenkinson H, Parulekar M, Wilson M, Peet AC, et al. , Metabolite profiling in retinoblastoma identifies novel clinicopathological subgroups, Br. J. Cancer 113 (2015) 1216–1224. [PubMed: 26348444]

[3]. Kohe SE, Bennett CD, Gill SK, Wilson M, McConville C, Peet AC, Metabolic profiling of the three neural derived embryonal pediatric tumors retinoblastoma, neuroblastoma and

medulloblastoma, identifies distinct metabolic profiles, Oncotarget 9 (2018) 11336–11351. [PubMed: 29541417]

[4]. Castelli V, Paladini A, d'Angelo M, Allegretti M, Mantelli F, Brandolini L, et al. , Taurine and oxidative stress in retinal health and disease, CNS Neurosci. Ther 27 (2021) 403–412. [PubMed: 33621439]

[5]. Heck JE, Lombardi CA, Meyers TJ, Cockburn M, Wilhelm M, Ritz B, Perinatal characteristics and retinoblastoma, Cancer Causes Control 23 (2012) 1567–1575. [PubMed: 22843021]

[6]. He D, Yan Q, Uppal K, Walker DI, Jones DP, Ritz B, et al. , Metabolite stability in archived neonatal dried blood spots used for epidemiological research, Am. J. Epidemiol 192 (2023) 1720–1730. [PubMed: 37218607]

[7]. Go Y-M, Walker DI, Liang Y, Uppal K, Soltow QA, Tran V, et al. , Reference standardization for mass spectrometry and high-resolution metabolomics applications to exposome research, Toxicol. Sci 148 (2015) 531–543. [PubMed: 26358001]

[8]. Deng K, Zhang F, Tan Q, Huang Y, Song W, Rong Z, et al. , WaveICA: a novel algorithm to remove batch effects for large-scale untargeted metabolomics data based on wavelet analysis, Anal. Chim. Acta 1061 (2019) 60–69. [PubMed: 30926040]

[9]. Saccenti E, Hoefsloot HCJ, Smilde AK, Westerhuis JA, Hendriks MMWB, Reflections on univariate and multivariate analysis of metabolomics data, Metabolomics 10 (2014) 361–374.

[10]. Wold S, Sjöström M, Eriksson L, PLS-regression: a basic tool of chemometrics, Chemom. Intell. Lab. Syst 58 (2001) 109–130.

[11]. Cocchi M, Biancolillo A, Marini F, Chapter Ten - Chemometric Methods for Classification and Feature Selection, in: Jaumot J, Bedia C, Tauler R (Eds.), Comprehensive Analytical Chemistry, Elsevier, 2018, pp. 265–299.

[12]. Bunin GR, Meadows AT, Emanuel BS, Buckley JD, Woods WG, Hammond GD, Pre- and postconception factors associated with sporadic heritable and nonheritable retinoblastoma, Cancer Res 49 (1989) 5730–5735. [PubMed: 2790788]

[13]. Heck JE, Omidakhsh N, Azary S, Ritz B, von Ehrenstein OS, Bunin GR, et al. , A case-control study of sporadic retinoblastoma in relation to maternal health conditions and reproductive factors: a report from the Children's Oncology Group, BMC Cancer 15 (2015), 735. [PubMed: 26481585]

[14]. Yost K, Perkins C, Cohen R, Morris C, Wright W, Socioeconomic status and breast cancer incidence in California for different race/ethnic groups, Cancer Causes Control 12 (2001) 703–711. [PubMed: 11562110]

[15]. Kato MV, Ishizaki K, Shimizu T, Ejima Y, Tanooka H, Takayama J, et al. , Parental origin of germ-line and somatic mutations in the retinoblastoma gene, Hum. Genet 94 (1994) 31–38. [PubMed: 8034292]

[16]. Liu KH, Nellis M, Uppal K, Ma C, Tran V, Liang Y, et al. , Reference standardization for quantification and harmonization of large-scale metabolomics, Anal. Chem 92 (2020) 8836–8844. [PubMed: 32490663]

[17]. Schrimpe-Rutledge AC, Codreanu SG, Sherrod SD, McLean JA, Untargeted metabolomics strategies-challenges and emerging directions, J. Am. Soc. Mass Spectrom 27 (2016) 1897–1905. [PubMed: 27624161]

[18]. Li S, Park Y, Duraisingham S, Strobel FH, Khan N, Soltow QA, et al. , Predicting Network Activity from High Throughput Metabolomics, PLOS Comput. Biol 9 (2013), e1003123. [PubMed: 23861661]

[19]. Tang X-H, Gudas LJ, Retinoids, retinoic acid receptors, and cancer, Annu. Rev. Pathol.: Mech. Dis 6 (2011) 345–364.

[20]. Lauritzen L, Brambilla P, Mazzocchi A, Harsløf LB, Ciappolino V, Agostoni C, DHA effects in brain development and function, Nutrients 8 (2016).

[21]. Campoy C, Escolano-Margarit MV, Anjos T, Szajewska H, Uauy R, Omega 3 fatty acids on child growth, visual acuity and neurodevelopment, Br. J. Nutr 107 (Suppl 2) (2012) S85–S106. [PubMed: 22591907]

[22]. Glatz JF, Luiken JJ, Fatty acids in cell signaling: historical perspective and future outlook, Prostaglandins Leukot. Ess. Fat. Acids 92 (2015) 57–62.

[23]. Richieri GV, Kleinfeld AM, Unbound free fatty acid levels in human serum, J. Lipid Res 36 (1995) 229–240. [PubMed: 7751810]

[24]. Mashima R, Okuyama T, The role of lipoxygenases in pathophysiology; new insights and future perspectives, Redox Biol 6 (2015) 297–310. [PubMed: 26298204]

[25]. Ying L, Marino J, Hussain SP, Khan MA, You S, Hofseth AB, et al. , Chronic Inflammation Promotes Retinoblastoma Protein Hyperphosphorylation and E2F1 Activation, Cancer Res 65 (2005) 9132–9136. [PubMed: 16230367]

[26]. Yan Q, Paul KC, Walker DI, Furlong MA, Del Rosario I, Yu Y, et al. , High-resolution metabolomic assessment of pesticide exposure in central valley, California, Chem. Res. Toxicol (2021).

[27]. Yan Q, Liew Z, Uppal K, Cui X, Ling C, Heck JE, et al. , Maternal serum metabolome and traffic-related air pollution exposure in pregnancy, Environ. Int 130 (2019), 104872. [PubMed: 31228787]

[28]. Heck JE, Wu J, Lombardi C, Qiu J, Meyers TJ, Wilhelm M, et al. , Childhood cancer and traffic-related air pollution exposure in pregnancy and early life, Environ. Health Perspect 121 (2013) 1385–1391. [PubMed: 24021746]

[29]. Ghosh JK, Heck JE, Cockburn M, Su J, Jerrett M, Ritz B, Prenatal exposure to traffic-related air pollution and risk of early childhood cancers, Am. J. Epidemiol 178 (2013) 1233–1239. [PubMed: 23989198]

[30]. Yin J, Ren W, Huang X, Deng J, Li T, Yin Y, Potential mechanisms connecting purine metabolism and cancer therapy, Front. Immunol 9 (2018).

[31]. Di Virgilio F, Adinolfi E, Extracellular purines, purinergic receptors and tumor growth, Oncogene 36 (2017) 293–303. [PubMed: 27321181]

[32]. Ganguly A, Shields CL, Differential gene expression profile of retinoblastoma compared to normal retina, Mol. Vis 16 (2010) 1292–1303. [PubMed: 20664703]

[33]. Dewett D, Lam-Kamath K, Poupault C, Khurana H, Rister J, Mechanisms of vitamin A metabolism and deficiency in the mammalian and fly visual system, Dev. Biol 476 (2021) 68–78. [PubMed: 33774009]

[34]. Buck J, Derguini F, Levi E, Nakanishi K, Hammerling U, Intracellular signaling by 14-hydroxy-4,14-retro-retinol, Science 254 (1991) 1654–1656. [PubMed: 1749937]

[35]. Sommer A, Tarwotjo I, Hussaini G, Susanto D, Increased mortality in children with mild vitamin A deficiency, Lancet 2 (1983) 585–588. [PubMed: 6136744]

[36]. Kim Y-K, Hammerling U, The mitochondrial PKCδ/retinol signal complex exerts real-time control on energy homeostasis, Biochim. Et. Biophys. Acta (BBA) - Mol. Cell Biol. Lipids 1865 (2020), 158614.

[37]. Huang X, Hansen J, Lee P-C, Wu C-K, Federman N, Arah OA, et al. , Maternal diabetes and childhood cancer risks in offspring: two population-based studies, Br. J. Cancer 127 (2022) 1837–1842. [PubMed: 36088507]

[38]. Gelaleti RB, Damasceno DC, Lima PHO, Salvadori DMF, Calderon Id.M.P., Peraçoli JC, et al. , Oxidative DNA damage in diabetic and mild gestational hyperglycemic pregnant women, Diabetol. Metab. Syndr 7 (2015) 1. [PubMed: 25810781]

[39]. van Reyk DM, Gillies MC, Davies MJ, The retina: oxidative stress and diabetes, Redox Rep 8 (2003) 187–192. [PubMed: 14599341]

[40]. Mallipatna A, Marino M, Singh AD, Genetics of Retinoblastoma, Asia Pac. J. Ophthalmol 5 (2016) 260–264.

[41]. Schauer R, Sialic acids: fascinating sugars in higher animals and man, Zoology 107 (2004) 49–64. [PubMed: 16351927]

[42]. Haznadar M, Cai Q, Krausz KW, Bowman ED, Margono E, Noro R, et al. , Urinary metabolite risk biomarkers of lung cancer: a prospective cohort study, Cancer Epidemiol. Biomark. Prev 25 (2016) 978–986.

[43]. Krolikowski FJ, Reuter K, Waalkes TP, Sieber SM, Adamson RH, Serum sialic acid levels in lung cancer patients, Pharmacology 14 (1976) 47–51. [PubMed: 183223]

[44]. Mathé EA, Patterson AD, Haznadar M, Manna SK, Krausz KW, Bowman ED, et al. , Noninvasive urinary metabolomic profiling identifies diagnostic and prognostic markers in lung cancer, Cancer Res 74 (2014) 3259–3270. [PubMed: 24736543]

[45]. Liang D, Ladva CN, Golan R, Yu T, Walker DI, Sarnat SE, et al. , Perturbations of the arginine metabolome following exposures to traffic-related air pollution in a panel of commuters with and without asthma, Environ. Int 127 (2019) 503–513. [PubMed: 30981021]

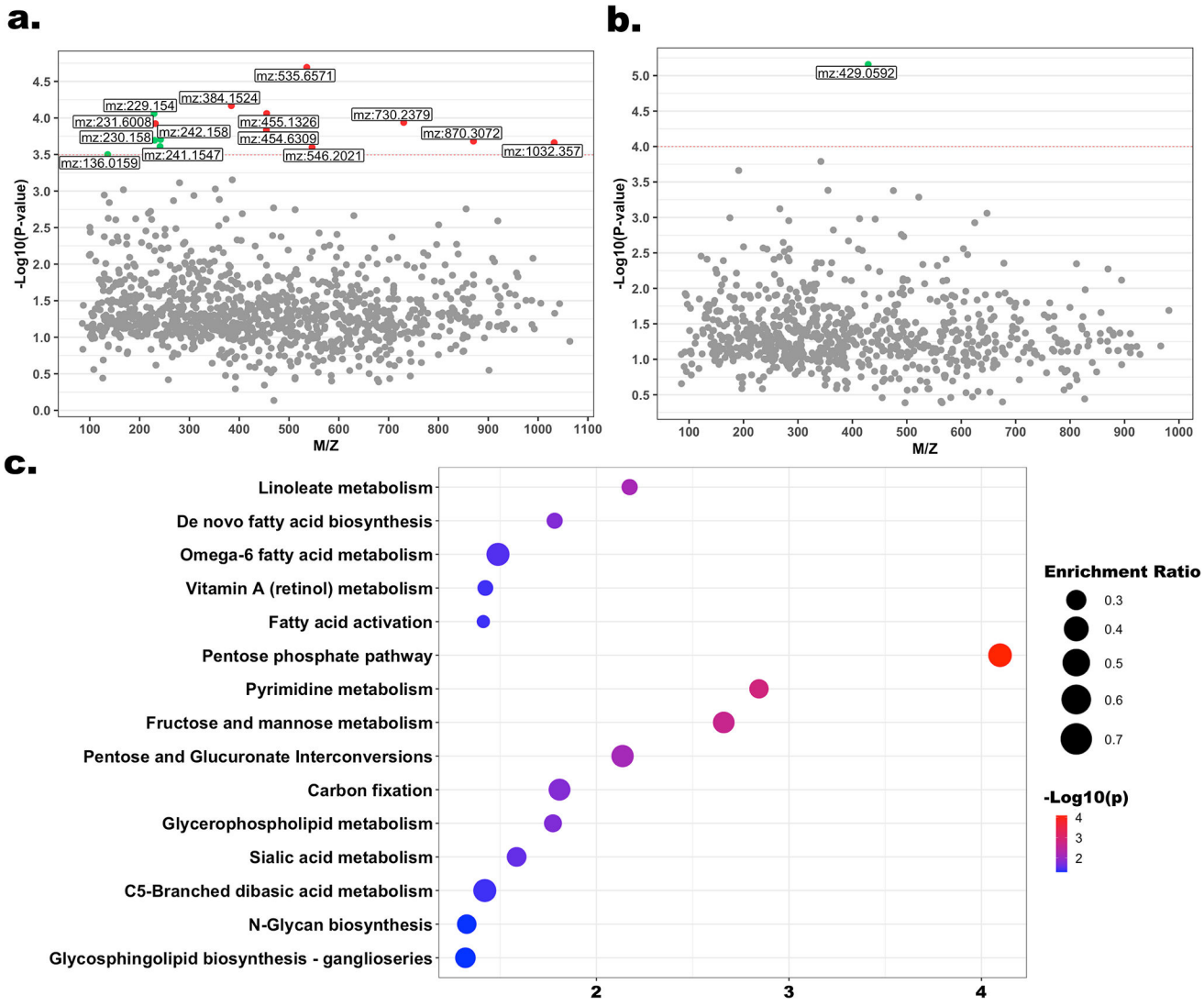

Fig. 1.

Metabolomic features and pathways associated with retinoblastoma status. (**a**) Type 1 Manhattan plot for features in the HILIC column (positive ion mode), −log10(p-value) vs mass-to-charge (*m/z*). Only features with VIP score > 1.5 were included here. 14 *m/z* features were found with FDR < 0.05. Red dots represent the features with higher intensities among cases, and the green dots represent the features with lower intensities among cases; **(b)** Type 1 Manhattan plot for features in the C18 column (negative ion mode), −log10(p-value) vs. mass-to-charge. 1 *m/z* feature was found with FDR < 0.05. Dot plot (**c**) shows the results of mummichog pathway enrichment analyses. X-axis represents −log10(*p-value*). The size of the dot represents the enrichment ratio.

Table 1

Demographic characteristics of the study population.

	Control (N = 853)	Case (N = 474)	
		Unilateral (N = 264)	Bilateral (N = 210)
Birth Year			
1983–2000	511 (59.9%)	157 (59.5%)	114 (54.3%)
2001–2003	110 (12.9%)	38 (14.4%)	30 (14.3%)
2004–2011	232 (27.2%)	69 (26.1%)	66 (31.4%)
Infant's Sex			
Male	419 (49.1%)	138 (52.3%)	118 (56.2%)
Female	434 (50.9%)	126 (47.7%)	92 (43.8%)
Preterm Birth			
Yes	84 (9.8%)	28 (10.6%)	28 (13.3%)
Foreign Born			
Yes	391 (45.8%)	119 (45.1%)	99 (47.1%)
Parity			
0	354 (41.5%)	97 (36.7%)	86 (41.0%)
1	254 (29.8%)	73 (27.7%)	61 (29.0%)
≥ 2	245 (28.7%)	94 (35.6%)	63 (30.0%)
Maternal Age			
< 20	95.0 (11.1%)	24 (9.1%)	21 (10.0%)
20–24	210 (24.6%)	60 (22.7%)	43 (20.5%)
25–29	229 (26.8%)	91 (34.5%)	59 (28.1%)
30–34	206 (24.2%)	56 (21.2%)	52 (24.8%)
> =35	113 (13.2%)	33 (12.5%)	35 (16.7%)
Maternal Race/Ethnicity			
White non-Hispanics	289 (33.9%)	78 (29.5%)	66 (31.4%)
Hispanic of any race	403 (47.2%)	123 (46.6%)	102 (48.6%)
Other/not specified	161 (18.9%)	63 (23.9%)	42 (20.0%)
Census-Based nSES Index Level			
1 (Low)	191 (22.4%)	68 (25.8%)	50 (23.8%)
2	237 (27.8%)	59 (22.3%)	58 (27.6%)
3	185 (21.7%)	57 (21.6%)	39 (18.6%)
4	128 (15.0%)	48 (18.2%)	42 (20.0%)
5 (High)	112 (13.1%)	32 (12.1%)	21 (10.0%)
Maternal Education			
Less than high school	240 (32.2%)	65 (27.5%)	68 (34.7%)
High school graduate	226 (30.3%)	75 (31.8%)	51 (26.0%)
Some college, college graduate or more	279 (37.4%)	96 (40.7%)	77 (39.3%)
Missing	108	28	14
Paternal Age			
< 20	30 (3.7%)	9 (3.6%)	9 (4.5%)

	Control (N = 853)	Case (N = 474)	
		Unilateral (N = 264)	Bilateral (N = 210)
20–24	166 (20.7%)	46 (18.3%)	26 (13.1%)
25–29	202 (25.2%)	64 (25.4%)	38 (19.2%)
30–34	192 (23.9%)	60 (23.8%)	55 (27.8%)
>=35	213 (26.5%)	73 (29.0%)	70 (35.4%)
Missing	50	12	12
Paternal Education			
Less than high school	202 (28.9%)	62 (27.7%)	57 (30.8%)
High school graduate	218 (31.2%)	74 (33.0%)	52 (28.1%)
Some college, college graduate or more	279 (39.9%)	88 (39.3%)	76 (41.2%)
Missing	154	40	25

Table 2

Confirmed [a] chemical identity of metabolic features associated with retinoblastoma status.

m/z	RT (s)	Adduct Form	Metabolite	Coefficient[b]	FDR	VIP	Mode
329.2478	24.0	M+H	Docosahexaenoic acid	0.162	0.101	2.248	HILICpos
301.2160	23.0	M+H	All-trans-Retinoic acid	0.152	0.105	1.996	HILICpos
118.0611	50.8	M+H	Guanidoacetic acid	0.119	0.105	1.772	HILICpos
332.5608	274.2	M+H	NAD	−0.110	0.106	1.717	HILICpos
689.2114	241.3	M+Na	Glycogen	−0.106	0.106	1.548	HILICpos
182.0811	46.0	M+H	L-Tyrosine	−0.107	0.106	1.544	HILICpos
290.1346	62.4	M+H	Ophthalmic acid	−0.102	0.110	1.605	HILICpos
137.1073	26.2	M+H	N,N-Dimethyl-1,4-Phenylenediamine	−0.089	0.142	1.645	HILICpos
442.0178	18.4	M-H	Guanosine diphosphate	−0.193	0.072	2.929	C18neg
489.9907	27.0	M-H	Deoxyadenosine triphosphate	−0.186	0.089	2.911	C18neg
604.0710	17.1	M-H	Guanosine diphosphate mannose	−0.179	0.089	2.681	C18neg
275.0180	17.0	M-H	6-Phosphogluconic acid	−0.183	0.089	2.825	C18neg
163.0400	26.4	M-H	Phenylpyruvic acid	−0.178	0.089	2.536	C18neg
362.0517	18.0	M-H	Guanosine monophosphate	−0.165	0.089	2.501	C18neg
309.2803	291.2	M-H	11Z-Eicosenoic acid	−0.167	0.100	2.399	C18neg
132.0303	20.1	M-H	D-Aspartic acid	−0.141	0.100	2.128	C18neg
331.2648	267.5	M-H	Adrenic acid	0.143	0.100	2.187	C18neg
176.0390	18.4	M-H	N-Formyl-L-methionine	−0.132	0.102	2.035	C18neg
304.0348	18.4	M-H	Cytidine 2’,3’-cyclic phosphate	0.126	0.102	1.823	C18neg
140.0829	19.3	M-H	L-Histidinol	0.117	0.102	1.717	C18neg
482.9601	18.5	M-H	Uridine triphosphate	−0.114	0.102	1.919	C18neg
140.0118	25.5	M-H	O-Phosphoethanolamine	−0.110	0.107	1.666	C18neg
190.0546	18.8	M-H	N-Acetyl-L-methionine	0.099	0.113	1.516	C18neg
147.0300	18.3	M-H	Citramalic acid	−0.095	0.124	1.686	C18neg
253.2177	236.7	M-H	Palmitoleic acid	0.100	0.125	1.676	C18neg
306.0500	17.9	M-H	dCMP	−0.098	0.131	1.620	C18neg
579.0279	16.8	M-H	Uridine diphosphate glucuronic acid	−0.094	0.133	1.500	C18neg
281.2491	274.7	M-H	Oleic acid	0.092	0.139	1.582	C18neg

[a] Chemical identification was conducted by matching peaks by accurate mass and retention time to authentic reference standards in an in-house library run under identical conditions using tandem mass spectrometry.

[b] Coefficients were derived from logistic regression, adjusted for potential confounders. A positive coefficient means that the metabolite level is higher among cases; a negative coefficient means that the metabolite level is lower among cases.